The Second TSME International Conference on Mechanical Engineering
19-21 October, 2011, Krabi

Numerical Study of the Heat Transfer Characteristics of a Turbulent Jet Impinging on a Cylindrical Pedestal

Mohammad Moghiman[1], Maryam Moein-far[2]* Rasool Elahi[3] and Morteza Abdollahian[4,]

[1,2,3,4] Department of Mechanical Engineering, Faculty of Engineering, Ferdowsi university of Mashhad, Mashhad, Iran 91775-1111

* Corresponding Author: Tel: +989375371702

E-mail: moeinfar.m@gmail.com

Abstract

In this paper the three dimensional round jet impinging on a circular pedestal is simulated. The predictions are carried out through numerical procedure based on finite volume method. The effects of the nozzle to target spacing (H/D=2, 4 and 6) and Reynolds numbers (23000 and 50000) are investigated. The flow field is considered to be incompressible and the buoyancy and radiation heat transfer effects are neglected. Turbulent fluctuations in the velocity field are modeled using the Reynolds Averaged Navier-Stokes (RANS) methodology and various turbulence models such as $SST\ k-\omega$, $RNG\ k-\varepsilon$, *Realizable* $k-\varepsilon$ and v^2-f are also used. The results of convective heat transfer obtained on the pedestal and the flat plate, using v^2-f turbulence model have good agreement with the experimental data compared to the other models and also heat transfer increases with increasing Reynolds number and the maximum heat transfer coefficients occur for H/d equals to six.

Keywords: *Turbulent impinging jet - Cylindrical pedestal - Numerical simulation - Heat transfer characteristics.*

1. Introduction

The impinging jet is used in many engineering and industrial applications such as annealing of metal and glass, cooling of cast iron and transistors, forming of plastic [1], drying film and textile [2], grinding processes [3], cooling of gas turbine blades [4-6] and cooling of microelectronic equipments [7, 8]. The high heat transfer rate generated by turbulent impinging jet flows is present even in aircraft industry, for example the flow field generated by the fan-powered vertical take-off and landing vehicles can be simulated and studied by considering the impinging jet flows [9]. These applications are due to the high heat and mass transfer rates of the jet impingement.

To design and optimize the jet impingement cooling, it is essential to determine and understand the effects of such important parameters as nozzle to plate distance, jet Reynolds number, Prandtl number, jet diameter, impact angle, nozzle geometry, confinement effect and etc. In some of previous studies these effects have been examined.

Basic features of such flows are different flow areas which are the area of free jets, the area of the gradient flow in the zone of critical point and the jet turn and the area of wall jet. The high

rate of heat and mass transfer processes in the stagnation region of the jet.

The impinging jet flow, despite its relatively simple geometry, exhibits extremely complex flow characteristics. Therefore it is a challenging case for turbulence models.

There have been numerous experimental and numerical investigations on the flow and heat transfer characteristics of the impinging jets, for example Mesbah [10] and Choi et al. [11] have studied the heat transfer of the circular jet on the concave surfaces experimentally. They concluded that the heat transfer at the stagnation point was increased with increasing relative surface curvature and was relatively higher than for an equivalent jet impinging on a flat plate. The effects of an isolated jet impinging on a circular pedestal have been also investigated experimentally by Parneix et al. [12], they found that the local Nusselt number distribution was different from the flat plate configuration since the stagnation Nusselt number was a local minimum. Lee [2] investigated the effect of the aspect ratio of the elliptic jets on the turbulent jet structure and heat transfer on the stagnation region of the plate. Esposito [6] studied two different styles of jet impingement geometries to be used in backside combustor cooling. There have been also many studies in trying to numerically predict the flow and heat transfer from the impingement of a jet, for example Behnia et al. [13] and Park and Sung [14] have computed the heat transfer from a turbulent impinging jet. Merci et al. [15] studied the heat transfer characteristics of an axisymmetric jet impinging on a cylindrical pedestal both experimentally and numerically. The unsteady simulations of a slot jet impinging normally onto a flat surface have been performed by Cziesla et al [16] using the large eddy simulation (LES) methodology and Chung et at [17] using direct numerical simulation (DNS). Rundstrom et al. [18] compared the performance of the $v^2 - f$ and the RSM turbulence models with a two-layer wall treatment for the prediction of the mean velocity field, the turbulence characteristics and the heat transfer rate of the normal impinging jet and also impinging jet in a cross-flow configuration.

In the present study a jet with various jet to plate distances at different Reynolds numbers, impinging on a circular pedestal is investigated numerically. The turbulence models such as $SST\ k-\omega$, $RNG\ k-\varepsilon$, $Realizable\ k-\varepsilon$ and $v^2 - f$ have also been used

2. Governing Equations

In this study, the flow field can be considered to be incompressible. The buoyancy and radiation heat transfer effects are neglected. The velocity and pressure have been decomposed into the mean and fluctuating components. The continuity equation is:

$$\frac{\partial U_i}{\partial x_i} = 0 \qquad (1)$$

Where U_i is the average of the velocity components. Assuming constant fluid properties, the momentum and energy equations are decoupled and the full momentum and energy equations are written in tensor forms as:

$$\frac{\partial U_i}{\partial t} + U_j \frac{\partial U_i}{\partial x_j} = -\frac{\partial P}{\partial x_i} + \nu \frac{\partial}{\partial x_j}\frac{\partial U_i}{\partial x_j} - \frac{\partial \overline{u_i' u_j'}}{\partial x_j} \qquad (2)$$

$$\frac{\partial T}{\partial t}+U_j\frac{\partial T}{\partial x_j}=\alpha\frac{\partial}{\partial x_j}\frac{\partial T}{\partial x_j}-\frac{\partial \overline{u_j'T'}}{\partial x_j} \quad (3)$$

Where p, T, ν and ρ are the pressure, temperature, kinematic viscosity and the fluid density respectively.

$$\alpha=\frac{k}{\rho c_p} \quad (4)$$

k is the thermal conductivity of the fluid and c_p is the specific heat at constant pressure. $\overline{u_i'u_j'}$ is the kinematic form of the Reynolds stress tensor and $\overline{u_j'T'}$ is the turbulent heat flux. Using Boussinesq eddy-viscosity assumption, the Reynolds stresses are approximated as:

$$\overline{u_i'u_j'}=\nu_T\left(\frac{\partial U_i}{\partial x_j}+k\delta_{ij}\right) \quad (5)$$

ν_T is the eddy viscosity and k is the turbulent kinetic energy. To solve equation (3), the turbulent heat flux is related to the mean velocity field by using the Boussinesq approximation where

$$\overline{u_i'T'}=\frac{\nu_T}{\mathrm{Pr}_T}\frac{\partial T}{\partial x_i} \quad (6)$$

As, air is assumed to be the working fluid, the molecular Prandtl number is set to a constant value of 0.7. Viscous heating is neglected and a constant turbulent Prandtl number is introduced to model the turbulent heat flux,

$$k_T=\nu_T/\mathrm{Pr}_T \quad (7)$$

Values of Pr_T vary from 0.73 to 0.92. Here, a constant value of $\mathrm{Pr}_T=0.85$ has been used.

3. Numerical Method

In this investigation a three-dimensional grid, made up of approximately 2342375 cells has been used. A schematic of computational domain in which the flat plate and the pedestal can be seen, is shown in Fig. 1. The grids near the pedestal are also shown in Fig. 2.

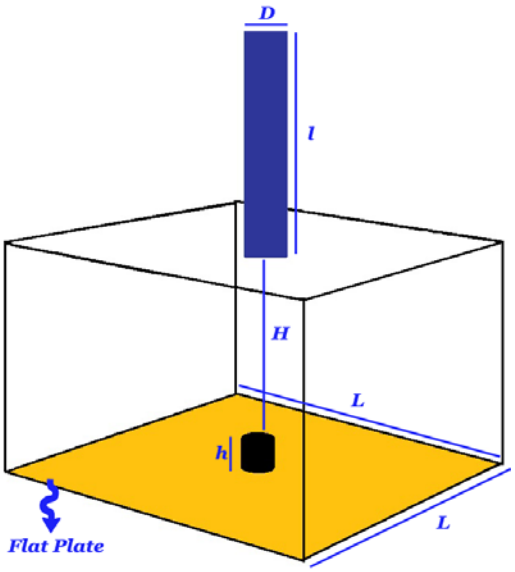

Fig. 1 The computational domain

D: The jet diameter

H: The jet to target distance

h: The height of the pedestal (h=2r=D/1.06 and r is the radius of the pedestal)

l: the jet length (it equals to six times of the jet diameter)

L: The flat plate length (it equals to ten times of the jet diameter)

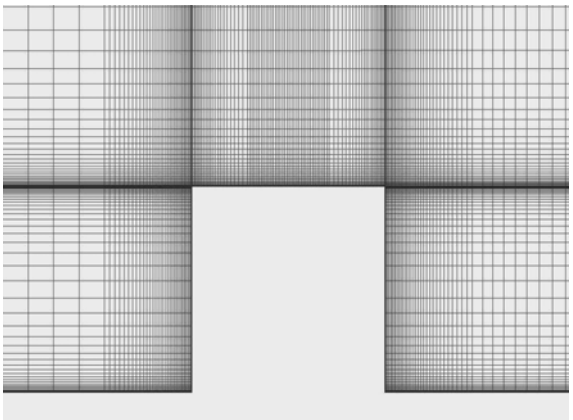

Fig. 2 The grids close to the pedestal

The numerical data for a round jet with different nozzle to target distances and various turbulence models at Reynolds numbers equal to 23000 and 50000 have been computed to

investigate the role of these parameters in predicting the flow and heat transfer characteristics of a jet impinging normally on a circular pedestal of height (h) and radius equal to D/1.06 and h/2 respectively. The pedestal has been heated and mounted on a flat plate.

In order to validate the numerical method, the data of the steady-state simulations for H/D=6 (H is jet to target distance and D is the jet diameter.) at Re=23000 have been compared to the available experimental data. The Reynolds number is calculated using the bulk velocity U_b, and the diameter of the pipe (D). Then using the same method, the impinging jet with two other jet to target distances (H/D=2 and H/D=4) at Re=23000 and Re=50000 have been simulated.

The Turbulent fluctuations in the velocity field have been modeled using the RANS methodology. Wall effects have been approximated using various turbulence models such as $SST\ k-\omega$, $RNG\ k-\varepsilon$, *Realizable* $k-\varepsilon$ and v^2-f.

The grids have strong clustering close to the walls to ascertain that the first computational node is at y+ ~ 1.

The SIMPLE algorithm has been used to couple the velocity and the pressure field. The second-order upwind discretization method has been applied to the convective fluxes in the momentum, energy and turbulence equations. Fully developed nozzle-exit velocity profile is also assumed in this study.

4. Boundary Condition

At the inlet boundary (the velocity inlet) the temperature is T0 = 295.2K, with atmospheric static pressure, a turbulent intensity of 1% and a turbulent length scale equal to the nozzle diameter have been used. The uniform temperature 321.2K has been imposed on the pedestal and the flat plate. Velocity components and turbulent kinetic energy have been set to zero at the solid boundaries and a zero derivative has been used for the static pressure. At the upper boundary, atmospheric static pressure has been imposed and radial derivatives for the other quantities have been set to zero (pressure outlet condition).

5. Results and Discussion

Fig. 3 shows the velocity fields for the different jet to target distances which are illustrated by the contour plots of the velocity magnitude in the xy-plane.

The flow fields show a complex behavior around the pedestal. The fluid emanating from the jet decelerates in the axial direction at the top of the pedestal where a stagnating streamline is positioned on the symmetry axis. Then the flow turns sharply and forms a radial wall jet along the upper surface of the pedestal.

At the corner of the pedestal, the flow separates and reattaches downstream on the plate. It creates a recirculation region that has a significant effect on the wall heat transfer. After reattachment, the flow develops into a wall jet along the plate.

The contours of turbulent kinetic energy around the pedestal for different jet to target distances at Re=50000 are presented in Fig 4. The maximum value is near the pedestal top corner, due to the large turbulent shear stresses in the curved streamlines in that region.

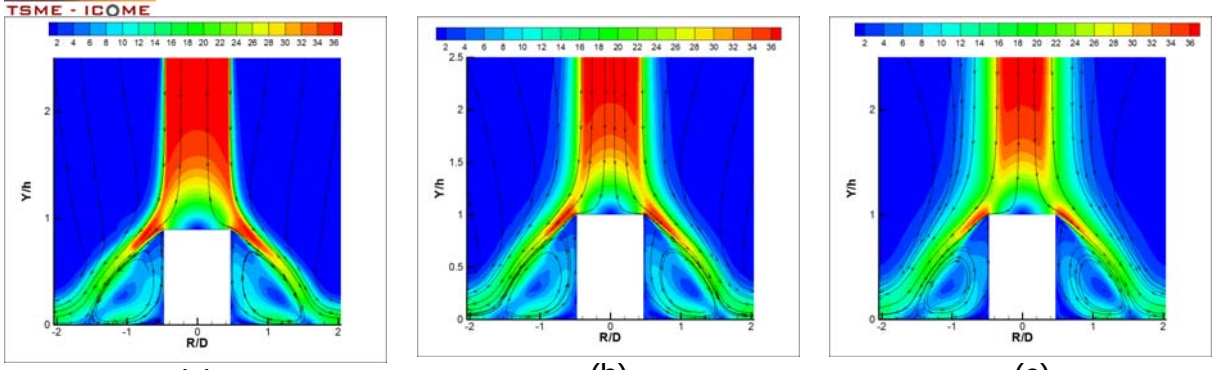

(a) (b) (c)

Fig. 3 Velocity contour around the pedestal ($\nu^2 - f$, Re=23000) (a- H/D=2, b-H/D=4, c-H/D=6)

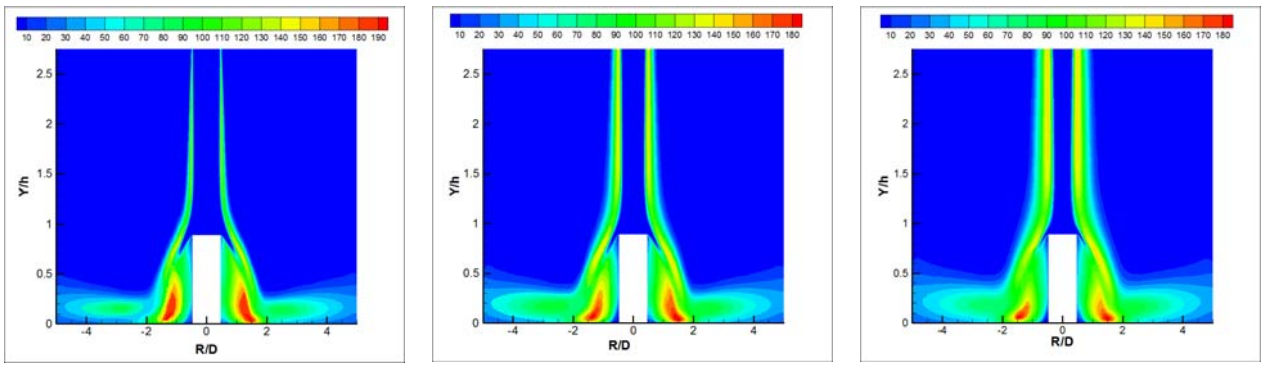

(a) (b) (c)

Fig. 4 Contour of turbulent kinetic energy around the pedestal ($\nu^2 - f$, Re=50000)

(a- H/D=2, b-H/D=4, c-H/D=6)

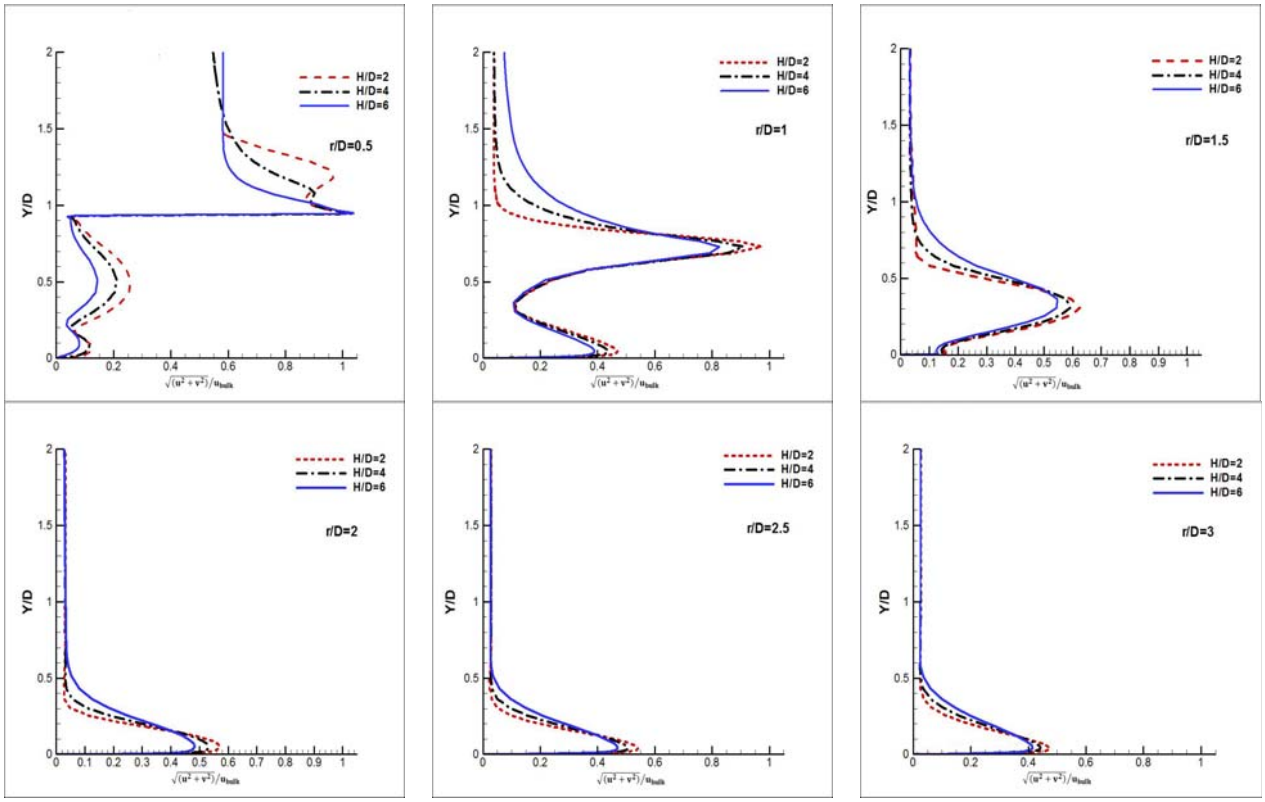

Fig. 5 Profiles of normalized velocity magnitude at different radial location ($\nu^2 - f$, Re=23000)

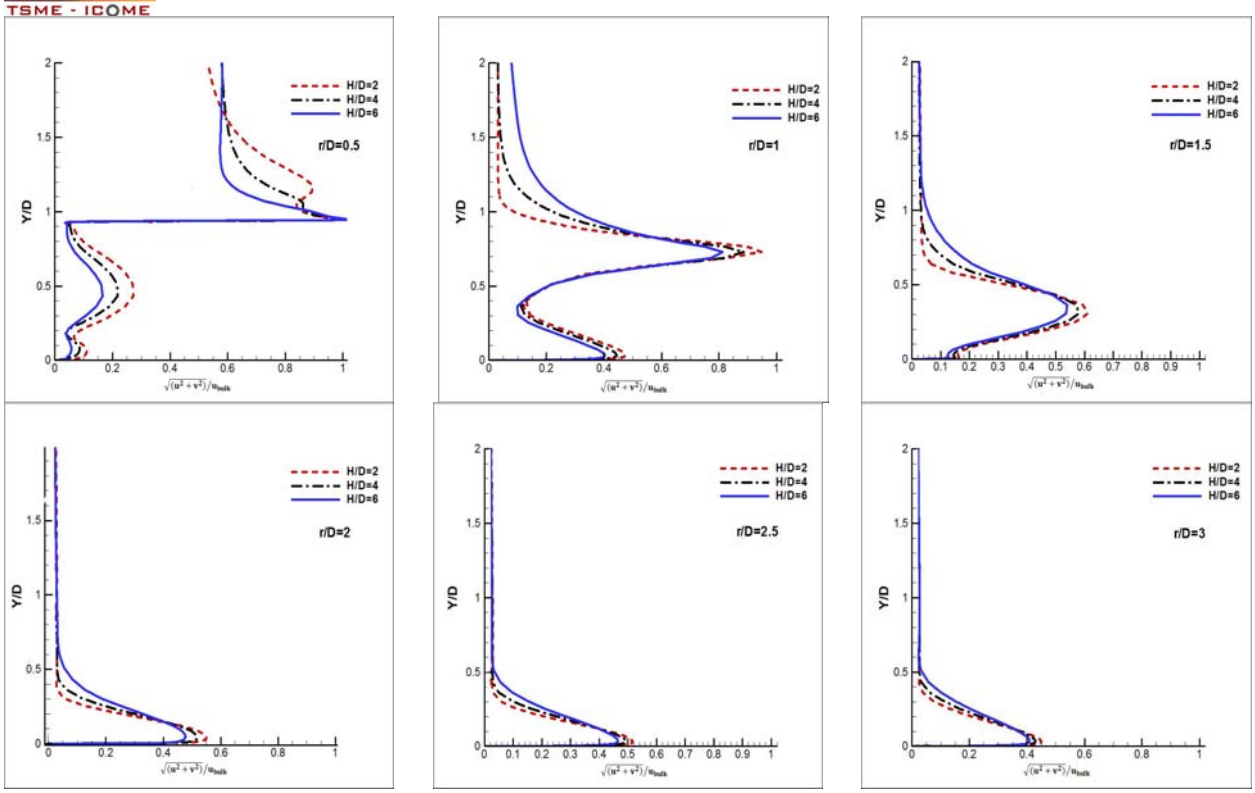

Fig. 6 Profiles of normalized velocity magnitude at different radial location (ν^2-f, Re=50000)

The non-dimensional velocity ($\sqrt{u^2+v^2}/U_{bulk}$) at Reynolds numbers equal to 23000 and 50000 at six different radial locations are presented in Figs 5 and 6 respectively. As it can be seen at r/D=2, 2.5 and 3 the non-dimensional velocity ($\sqrt{u^2+v^2}/U_{bulk}$) increases from a value of zero to a maximum and subsequently decays to a very small value. Figs 7 and 8 show the profiles for the surface heat transfer coefficient along the top face of the pedestal and the flat plate respectively. Data from the numerical predictions are validated against the experimental data reported by Mesbah [10]. These figures show that the *Realizable* $k-\varepsilon$ prediction is more than 100% higher than the experimental values and with the SST $k-\omega$ model, heat transfer coefficients are underpredicted while with two $k-\varepsilon$ models especially with *Realizable* $k-\varepsilon$ model, they are overpredicted. This is in accordance with the higher level of turbulent kinetic energy with this model. On the other hand, numerical predictions obtained using the ν^2-f turbulence model are in good agreement with the experimental data, both qualitatively and quantitatively. The results show a local minimum in the heat transfer coefficient on the symmetry axis, which is in contrast to observations on a simple flat plate.

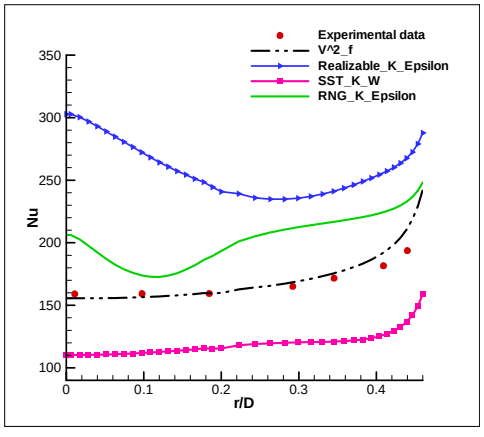

Fig. 7 Profiles of surface heat transfer coefficient along the pedestal top face (H/D=6, Re=23000)

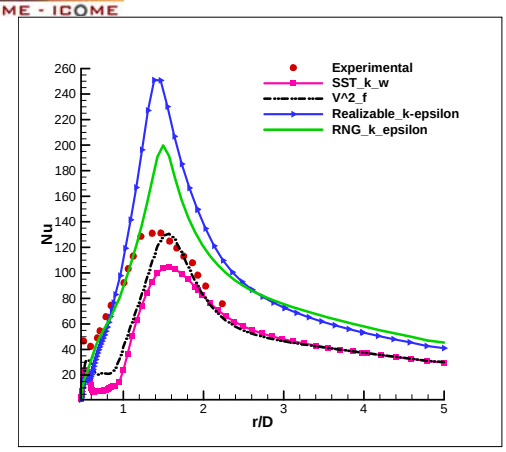

Fig. 8 Profiles of surface heat transfer coefficient along the flat plate (H/D=6, Re=23000)

The profiles of the surface heat transfer coefficient along the top face of the pedestal at different jet to target distances, are shown in Figs 9 and 10 at Reynolds numbers equal to 23000 and 50000 respectively. As it can be seen, in these figures, by increasing Reynold number, the momentum of the flow would be increased and the circular shape of the impinging jet would preserved for different H/D. For low Reynold number, the momentum of the flow would be diffused easily and the flow regime would be changed for different H/D. Consequently for low Reynolds impinging jet, variation of Nu number are larger than high Reynolds impinging jet.

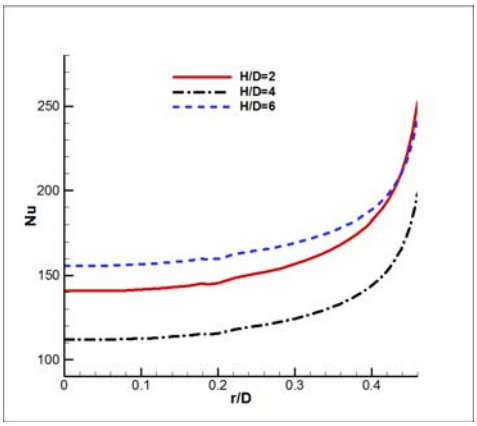

Fig. 9 Profiles of surface heat transfer coefficient along the pedestal top face ($\nu^2 - f$, Re=23000)

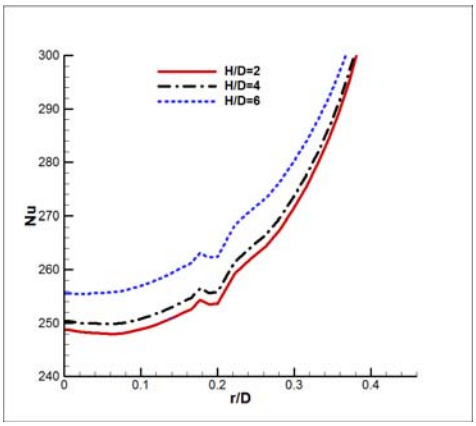

Fig. 10 Profiles of heat transfer coefficient along the pedestal top face ($\nu^2 - f$, Re=23000)

Figs 11 and 12 also show the heat transfer coefficient along the flat plate at different jet to target distances for both Reynolds numbers. According to these figures the maximum stagnation heat transfer coefficient occur for H/d equal to six and as the boundary layer thickness has been decreased by increasing the Reynolds number, and the heat transfer rate and consequently the Nuselt number would increase.

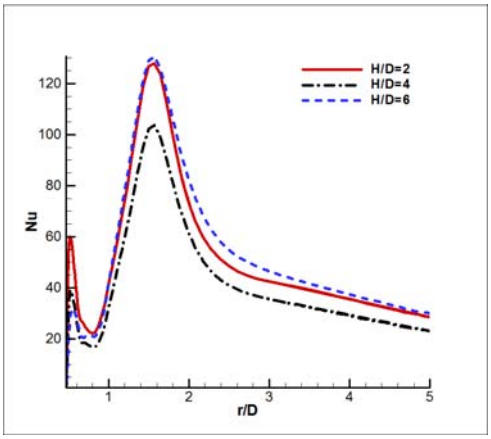

Fig. 11 Profiles of surface heat transfer coefficient along the flat plate ($\nu^2 - f$, Re=23000)

Reynolds number on the turbulence and the heat transfer characteristics. The results show that the local heat transfer coefficient on both the pedestal top surface and the plate are predicted with $\nu^2 - f$ turbulence model

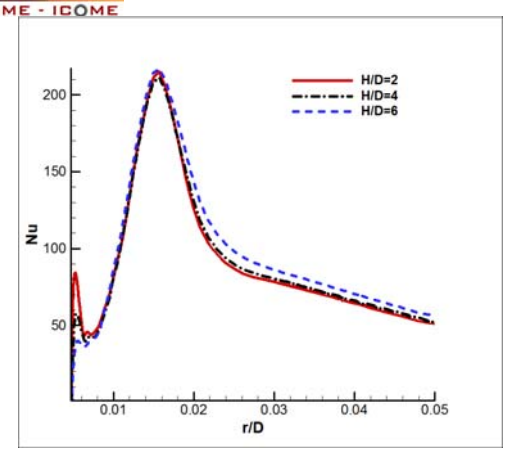

Fig. 12 Profiles of surface heat transfer coefficient along the flat plate(v^2-f,Re=50000)

Correctly and with the $SST\ k-\omega$ model, heat transfer coefficients are underpredicted while with both $k-\varepsilon$ models, they are overpredicted. So, the v^2-f model performs well for all cases. The investigation of heat transfer coefficients along the top surface of the pedestal and the flat plate show that the heat transfer increases with increasing Reynolds number and the maximum heat transfer coefficients belong to the nozzle to target distance equals to six times of the jet diameter.

7. References

[1] Abdel-Fattah, A. (2007). Numerical and experimental study of turbulent impinging twin-jet flow, *Experimental Thermal and Fluid Science*, vol.31, 2007, pp. 1061– 1072.

[2] Lee, J. and Lee, S. (2000). The effect of nozzle aspect ratio on stagnation region heat transfer characteristics of elliptic impinging jet, *International Journal of Heat and Mass Transfer*, vol.43, 2000, pp. 555– 575.

[3] Babic, D., Murray, D.B. and Torrance, A.A. (2005). Mist jet cooling of grinding processes, *Int. J. Mach. Tools Manufact*, vol.45, 2005, pp. 1171– 1177.

[4] Grady, J.O. (2007). Jet Impingement Cooling of Turbine Blades by Forced Convection, MAE 221A Heat Transfer, University of California, San Diego, Department of Mechanical and Aerospace Engineering, December 7.

[5] Liu, Q., Sleiti, A.K. and Kapat, J.S.(2008). Application of pressure and temperature sensitive paints for study of heat transfer to a circular impinging air jet, *International Journal of Thermal Sciences*, vol.47, 2008, pp. 749– 757.

[6] Esposito, E.I. (2006). Jet Impingement cooling configurations for gas turbine combustion, Master of Science in Mechanical Engineering, Mechanical Engineering Dept., Louisiana State Univ., Agricultural and Mechanical College.

[7] Kercher, D.S, Lee, J.B., Brand, O., Allen, M.G. and Glezer, A. (2003). Microjet cooling devices for thermal management of electronics, *Transactions of the ASME*, vol.125(2), 2003, pp. 359– 366.

[8] Cheng, T.C., Chiou, P.H. and Lin, T.F. (2002). Visualization of Mixed Convective Vortex Rolls in an Impinging Jet Flow of Air through a Cylindrical Chamber, *International Journal of Heat and Mass Transfer*, vol.45, 2002, pp. 3357– 3368.

[9] Siclari, M. and Migdal, D. (1976). Development of theoretical models for jet-induced effects on Vlstol aircraft, *Journal of Aircraft*, vol.13(12), 1976, pp. 938– 944.

[10] Mesbah, M. (1996). An Experimental Study of Local Heat Transfer to an Impinging Jet on Nonflat Surfaces: A Cylindrical Pedestal and a

Hemispherically Concave Surface, Ph.D thesis, University of California, Davis, CA.

[11] Choi, M., Yoo, H., Yang, G., J.S. Lee, J. and Sohn, D. (2000). Measurements of impinging jet flow and heat transfer on a semi-circular concave surface, *International Journal of Heat and Mass Transfer*, vol.43, 2000, pp. 1811– 1822.

[12] Parneix, S., Behnia, M.and Durbin, P. (1999). Predictions of turbulent heat transfer in an axisymmetric jet impinging on a heated pedestal, *ASME, Journal of heat transfer*, vol.121, 1999, pp. 43– 49.

[13] Behnia, M., Pameix, S., Shabany, Y. and Durbin, P. (1999). Numerical study of turbulent heat transfer in confined and unconfined impinging jets, *International journal of heat and fluid flow*, vol.20, 1999, pp. 1– 9.

[14] Park, T. and Sung, H. (2001). Development of a near-wall turbulence model and application to jet impingement heat transfer, *International journal of heat and fluid flow*, vol.22, 2001, pp. 10– 18.

[15] Merci, B., Mesbah, M.P.E., and Baughn, J.W. (2005). Experimental and numerical study of turbulent heat transfer on a cylindrical pedestal, *International journal of heat and fluid flow*, vol.26, 2005, pp. 233– 243.

[16] Cziesla, T., Biswas, G., Chattopadhyay, H. and Mitra, N. (2001). Large-eddy simulation of flow and heat transfer in an impinging slot jet, *International journal of heat and fluid flow*, vol. 22, 2001, pp. 500– 505

[17] Chung, Y. M., and Luo, K.H. (2002). Unsteady heat transfer analysis of an impinging jet, Journal of Heat Transfer, *Transactions of the ASME*, vol. 124, December 2002, pp. 1039– 1048.

[18] Rundstrom, D., Moshfegh, B., and Ooi, A. (2007). RSM and $v^2 - f$ Predictions of an Impinging Jet in a Cross Flow on a Heated Surface and on a Pedestal, paper presented in *the 16th Australasian Fluid Mechanics Conference* Crown Plaza, Gold Coast, Australia, December 2-7.